Supporting information for

Predicting pesticide fate in small cultivated mountain watersheds using the DynAPlus model: towards improved assessment of peak exposure

Melissa Morselli[1], Chiara Maria Vitale[1], Alessio Ippolito[2,3,§], Sara Villa[2], Roberto Giacchini[2], Marco Vighi[2,4], Antonio Di Guardo[1*]

[1]Department of Science and High Technology - University of Insubria, Via Valleggio 11, 22100 Como CO, Italy

[2]Department of Earth and Environmental Sciences, University of Milano-Bicocca, Piazza della Scienza 1, 20126 Milano MI, Italy

Current address:

[3]European Food Safety Authority (EFSA), Via Carlo Magno 1, 43125 Parma, Italy

[4]IMDEA Water Institute, Av.da Punto Com 2, 28805 Alcalà de Henares, Madrid, Spain

[§]Disclaimer - A. Ippolito is employed by the European Food Safety Authority. The positions and opinions presented in this article are those of the authors alone and do not necessarily represent the views or scientific works of the European Food Safety Authority

[*]Corresponding author. E-mail address: antonio.diguardo@uninsubria.it (A. Di Guardo).

Contains 8 texts, 16 figures, and 7 tables

MATERIALS AND METHODS

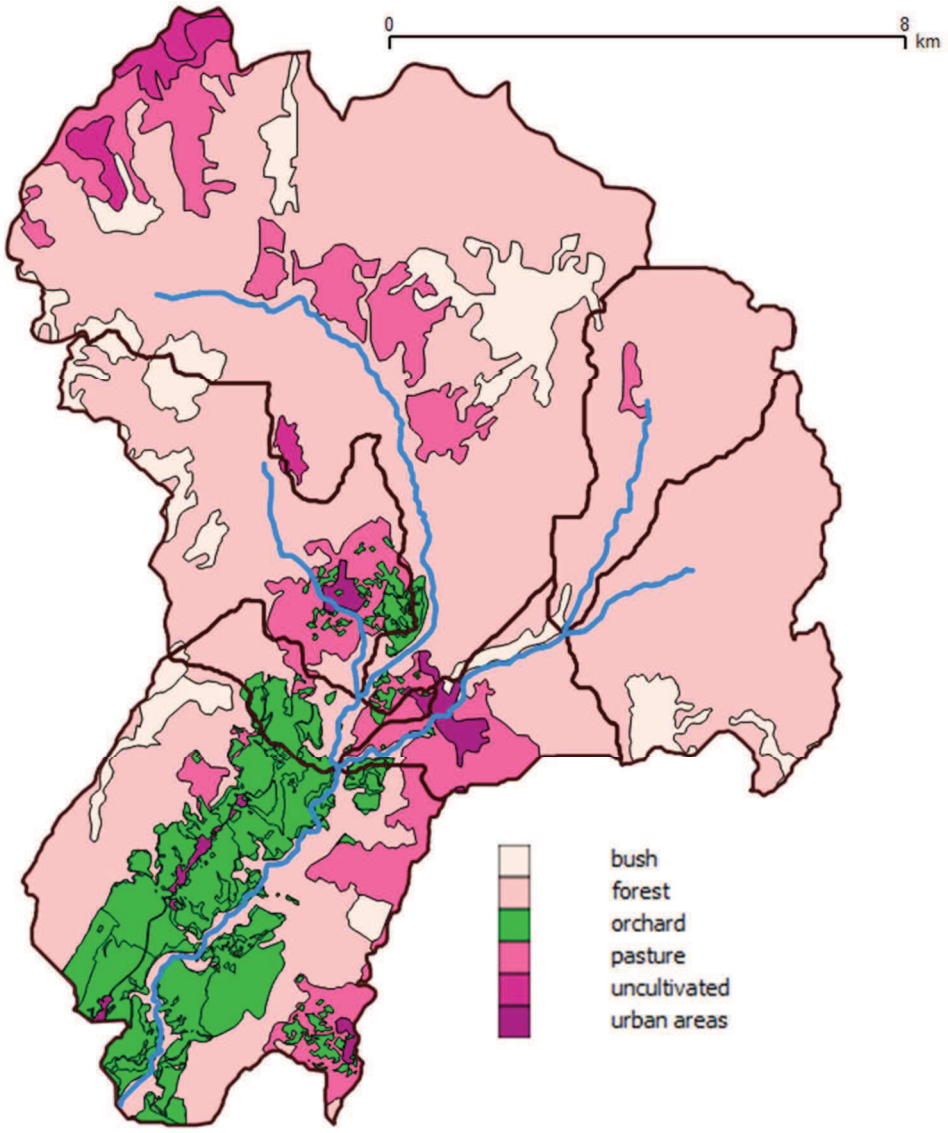

Figure S1. Main land use types in the Novella River watershed (ISPRA, 2017; GPTP, 2017; Google Maps, 2017).

Text S1 - SoilPlus improvements

In the present work, SoilPlus was improved by including (1) a slope-correction for curve number (CN), to allow a more accurate prediction of water (and thus chemical) runoff in slope conditions, and (2) a crop interception-washoff module for the calculation of canopy-mediated chemical loadings to soil.

Slope correction for curve number

The traditional CN approach does not account for the effect of slope when calculating the amount of runoff water and was developed for slopes < 5% (SCS, 1972), while in the Novella watershed slopes are on average ~ 30%, with maxima up to 80% (Trento Province, 2017). Three empirical approaches from the literature were implemented in SoilPlus and tested: the CN slope-correction reported in Sharpley and Williams (1990), the Sharpley and Williams correction optimized by Huang et al. (2006), and a third relationship developed by Huang et al. (2006) starting from their own dataset. The integrated model (SoilPlus + DynANet) was run using the three approaches for the period July-October 2009, for which discharge records measured in the Novella River were available (Biasioni, 2010). The comparison between predictions and observations showed improved model performance for all approaches, with the original Sharpley and Williams (1990) producing the best fit (results not shown). Such CN slope-correction was therefore selected for runoff simulations in the Novella River case study. According to Sharpley and Williams (1990), the CN for average moisture conditions (i.e., CN2), attributed to a given soil according to hydrological group and land use, should be corrected as follows:

$$CN_{2s} = \frac{1}{3}\left(CN_3 - CN_2\right)\left[1 - 2 \cdot exp(-13.86 \cdot Slp)\right] + CN_2 \qquad (1)$$

where *CN2s* is the slope-corrected CN_2, CN_2 is the tabulated CN for average moisture conditions, CN_3 is the CN for wet moisture conditions, and *Slp* (m m^{-1}) is slope.

Crop interception-washoff module

In the present version of the integrated model, a crop interception-washoff module was implemented on the grounds of FOCUS (2001a). Calculations are performed on a daily basis to provide the amount of pesticide transferred from leaves to soil via washoff. Washoff from plant surfaces is modelled using a relationship based on the pesticide mass on leaves, a washoff coefficient related to chemical water-solubility and rainfall amount. The chemical mass available on foliage after rainfall (*M*, mg) is calculated as follows:

$$M = M_0 \cdot exp(-Fextr \cdot Rain) \quad (2)$$

where M_0 (mg) is the chemical mass on foliage before rainfall, *Fextr* (mm^{-1}) is the foliar extraction coefficient and *Rain* (mm) is the daily rainfall amount. *Fextr* is in turn calculated as:

$$Fextr = 0.016 \cdot WS^{0.3832} \quad (3)$$

where *WS* (mg L^{-1}) is the chemical aqueous solubility. Although a crop compartment was not included in the SoilPlus model (i.e., crop does not participate to chemical mass balance in other compartments except for washoff and concentrations in foliage are not influenced by other compartments), the amount of chemical subtracted to washoff via dissipation (degradation + volatilization) was calculated as first-order kinetics from foliar dissipation half-life, as reported in FOCUS (2001a). The full inclusion of a vegetation/crop compartment in the integrated model will be the object of future work.

Text S2 - Water-routing and connection between links

In DynANet river networks composed of stream links (i.e., segments) classified according to the Strahler stream order method (Strahler, 1952) can be modelled. Spatial information concerning the river network is loaded via a standard shapefile and the link properties (order, link length, bottom width, average slope, upstream/downstream connections) are read from the corresponding attribute table. Order-1 links are first extracted via a query engine and water and chemical calculations are performed; extraction and calculations for higher order links follow. Chemical is considered as "well mixed" in each stream link, and its concentration is therefore assumed as uniform. The different links are connected by water fluxes. A baseflow value is input to order-1 links and then routed to higher-order ones; all the other water inputs for each segment (i.e., water runoff from the corresponding sub-basin and water coming from upstream links) are added to the top-end of the segment and subsequently routed through the segment length. Water movement is described using the variable storage routing method developed by Williams (1969); since the input data required by such procedure (i.e., rating curves at representative sections of the valley and hydrographs from the incremental areas) are seldom available for natural systems, the Manning's equation for uniform flow in a channel is used to compute the flow rate in the stream segment during the time step, as in the SWAT model (Neitsch et al., 2005). To account for slope, the correction to the Manning coefficient n (expressing friction) reported in Jarrett (1984) was implemented. A detailed description of DynANet model water and chemical routing equations follows, preceded by Table S1, listing all the variables involved.

Table S1. List of the variables involved in the water and chemical routing procedure.

Variable	Units	Description
Δt	h	Time step adopted for calculations (= 1 h)
AveVIn	m^3	Average inflow water volume during the time step
ChemRunoff	mol h^{-1}	Chemical entering the segment via runoff
ChemWat	mol	Chemical amount in water from upstream links
ChemPart	mol	Particle-bound chemical amount from upstream links
CLgth	m	Stream segment length
FlowArea	m^2	Stream cross-sectional area
FlowDepth	m	Stream depth
FlowRateMan	m^3 h^{-1}	Flow rate calculated with Manning's equation
HydrRad	m	Hydraulic radius
i	-	Julian hour
LINK	-	Segment ID in the attribute table
nMan	-	Manning's "n" coefficient for the stream
Qbase	m^3 h^{-1}	Baseflow
Qrunoff	m^3 h^{-1}	Inflow rate of runoff water
RoffWatSP	m^3	Hourly runoff water volume provided by SoilPlus
RoffChemSP	mol	Hourly runoff chemical amount provided by SoilPlus
SCoeff	-	Storage coefficient
slp	m m^{-1}	Average slope along the stream segment
SoilUseAn	m^2	Area occupied by soil type and use "n"
TTime	h	Travel time
USLINK	-	Upstream link segment ID in the attribute table
VIn	m^3	Volume of inflow water at the end of the time step (baseflow + runoff)
VInSto	m^3	Sum of the average inflow water volume during the time step and the volume of water stored at the end of the previous time step
VOutEnd	m^3	Volume of outflow water during the time step
VStoEnd	m^3	Volume of water stored at the end of the time step
VWat	m^3	Water volume in the stream segment
WatIn	m^3 h^{-1}	Inflow water rate
WatOut	m^3 h^{-1}	Outflow water rate
WatArea	m^2	Area of the water-air interface of the stream segment
Wbtm	m	Average stream bed width
WetP	m	Wetted perimeter
Zch	-	Inverse of channel side slope (e.g., 2 if side slope is 1/2)

Water routing procedure for each order-1 stream segment "LINK" (pseudo-code)

$$Qbase(LINK,i) = 600$$

$$Qrunoff(LINK,i) = RoffWatSP(LINK,i)$$

$$Vin(LINK,i) = (Qbase(LINK,i) + Qrunoff(LINK,i)) \cdot \Delta t$$

If i = 1 Then
$$Vin(LINK,i-1) = Vin(LINK,i)$$
End If

$$AveVin(LINK,i) = \frac{Vin(LINK,i) + Vin(LINK,i-1)}{2}$$

If i = 1 Then
$$VStoEnd(LINK,i-1) = 0$$
End If

$$VInSto(LINK,i) = AveVIn(LINK,i) + VStoEnd(LINK,i-1)$$

$$FlowArea(LINK,i) = \frac{VInSto(LINK,i)}{CLgth(LINK)}$$

$$FlowDepth(LINK,i) = \sqrt{\frac{FlowArea(LINK,i)}{Zch(LINK)} + \left(\frac{Wbtm(LINK)}{2 \cdot Zch(LINK)}\right)^2} - \frac{Wbtm(LINK)}{2 \cdot Zch(LINK)}$$

$$WetP(LINK,i) = Wbtm(LINK) + 2 \cdot FlowDepth(LINK,i) \cdot \sqrt{1 + Zch(LINK)^2}$$

$$HydrRad(LINK,i) = \frac{FlowArea(LINK,i)}{WetP(LINK,i)}$$

$$nMan(LINK) = 0.39 \cdot slp(LINK)^{0.38} \cdot HydrRad(LINK,i)^{-0.16}$$

$$FlowRateMan(LINK,i) = \frac{3600 \cdot FlowArea(LINK,i) \cdot HydrRad(LINK,i)^{2/3} \cdot slp(LINK)^{1/2}}{nMan(LINK)}$$

$$TTime(LINK,i) = \frac{CLgth(LINK) \cdot FlowArea(LINK,i)}{FlowRateMan(LINK,i)}$$

If $TTime(LINK, i) < 1$ Then
$$TTime(LINK,i) = 1$$
End If

$$SCoeff(LINK,i) = \frac{2 \cdot \Delta t}{2 \cdot TTime(LINK,i) + \Delta t}$$

If $SCoeff(LINK, i) > 1$ Then
$SCoeff(LINK,i) = 1$
End If

$$VOutEnd(LINK,i) = SCoeff(LINK,i) \cdot VInSto(LINK,i)$$

$$VStoEnd(LINK,i) = VStoEnd(LINK,i-1) + AveVIn(LINK,i) - VOutEnd(LINK,i)$$

$$FlowArea(LINK,i) = \frac{VStoEnd(LINK,i)}{CLgth(LINK)}$$

$$FlowDepth(LINK,i) = \sqrt{\frac{FlowArea(LINK,i)}{Zch(LINK)} + \left(\frac{Wbtm(LINK)}{2 \cdot Zch(LINK)}\right)^2} - \frac{Wbtm(LINK)}{2 \cdot Zch(LINK)}$$

Water volume, water fluxes, water surface and chemical loading via runoff

$$VWat(LINK,i) = VStoEnd(LINK,i)$$

$$WatIn(LINK,i) = AveVIn(LINK,i)$$

$$WatOut(LINK,i) = VOutEnd(LINK,i)$$

$$WatArea(LINK) = CLgth(LINK) \cdot Wbtm(LINK)$$

$$ChemRunoff(LINK,i) = RoffChemSP(LINK,i)$$

Water routing procedure for each higher order stream segment "LINK" with two upstream links "USLINK"

$$Qrunoff(LINK,i) = RoffWatSP(LINK,i)$$

$$Vin(LINK,i) = (VOutEnd(USLINK1,i) + VOutEnd(USLINK2,i) + Qrunoff(LINK,i)) \cdot \Delta t$$

If i = 1 Then
$Vin(LINK,i-1) = Vin(LINK,i)$
End If

$$AveVin(LINK,i) = \frac{Vin(LINK,i) + Vin(LINK,i-1)}{2}$$

$$VInSto(LINK,i) = AveVIn(LINK,i) + VStoEnd(LINK,i-1)$$

$$FlowArea(LINK,i) = \frac{VInSto(LINK,i)}{CLgth(LINK)}$$

$$FlowDepth(LINK,i) = \sqrt{\frac{FlowArea(LINK,i)}{Zch(LINK)} + \left(\frac{Wbtm(LINK)}{2 \cdot Zch(LINK)}\right)^2} - \frac{Wbtm(LINK)}{2 \cdot Zch(LINK)}$$

$$WetP(LINK,i) = Wbtm(LINK) + 2 \cdot FlowDepth(LINK,i) \cdot \sqrt{1 + Zch(LINK)^2}$$

$$HydrRad(LINK,i) = \frac{FlowArea(LINK,i)}{WetP(LINK,i)}$$

$$nMan(LINK) = 0.39 \cdot slp(LINK)^{0.38} \cdot HydrRad(LINK,i)^{-0.16}$$

$$FlowRateMan(LINK,i) = \frac{3600 \cdot FlowArea(LINK,i) \cdot HydrRad(LINK,i)^{2/3} \cdot slp(LINK)^{1/2}}{nMan(LINK)}$$

$$TTime(LINK,i) = \frac{CLgth(LINK) \cdot FlowArea(LINK,i)}{FlowRateMan(LINK,i)}$$

If $TTime(LINK, i) < 1$ Then
$TTime(LINK,i) = 1$
End If

$$SCoeff(LINK,i) = \frac{2 \cdot \Delta t}{2 \cdot TTime(LINK,i) + \Delta t}$$

If $SCoeff(LINK, i) > 1$ Then
$SCoeff(LINK,i) = 1$
End If

$$VOutEnd(LINK,i) = SCoeff(LINK,i) \cdot VInSto(LINK,i)$$

$$VStoEnd(LINK,i) = VStoEnd(LINK,i-1) + AveVIn(LINK,i) - VOutEnd(LINK,i)$$

$$FlowArea(LINK,i) = \frac{VStoEnd(LINK,i)}{CLgth(LINK)}$$

$$FlowDepth(LINK,i) = \sqrt{\frac{FlowArea(LINK,i)}{Zch(LINK)} + \left(\frac{Wbtm(LINK)}{2 \cdot Zch(LINK)}\right)^2} - \frac{Wbtm(LINK)}{2 \cdot Zch(LINK)}$$

Water volume, water fluxes, water surface and chemical loading via runoff and routing

$$VWat(LINK,i) = VStoEnd(LINK,i)$$

$$WatIn(LINK,i) = AveVIn(LINK,i)$$

$$WatOut(LINK,i) = VOutEnd(LINK,i)$$

$$WatArea(LINK) = CLgth(LINK) \cdot Wbtm(LINK)$$

$$ChemRunoff\,(LINK,i) = RoffChemSP(LINK,i)$$

$$ChemRouting(LINK,i) = ChemWat(USLINK1,i) + ChemWat(USLINK2,i) + \\ + ChemPart(USLINK1,i) + ChemPart(USLINK2,i))$$

Text S3 - Drift calculations and assumptions in DynANet

To account for direct chemical input via spray drift, the drift loading across the width of the different stream links (if surrounded by orchards) is calculated in DynANet as reported in FOCUS (2001a):

$$Drift = \left[\frac{A}{(B+1)} * [H^{B+1} - z_1{}^{B+1}] + \frac{C}{(D+1)} * [z_2{}^{D+1} - H^{D+1}] \right] * \frac{1}{z_2 - z_1} \quad (4)$$

where *Drift* is the mean percent drift loading across a water body extending from a distance of z_1 to z_2 from the edge of the treated field, z_1 (m) is the distance from edge of treated field to closest edge of water body, z_2 (m) is the distance from edge of treated field to farthest edge of water body, *A*, *B*, *C* and *D* are regression parameters, and *H* is the distance limit for each regression (m), also called hinge point. The percent drift calculated with Equation 4 is then converted into drift loading (*DLoad*; mg m^{-2}) using chemical application rate (*AppRate*, g ha^{-1}):

$$DLoad = \frac{AppRate}{10} \cdot \frac{Drift}{100} \quad (5)$$

Drift loading in mg m^{-2} is in turn multiplied by the stream area exposed to drift (m^2) to obtain the chemical amounts (mg) that are directly discharged into the modelled stream link during application days.

Assumptions and model parameterization for the Novella River case study

Since most of the apple orchards in the Novella River watershed (~ 85%) are located nearby stream link 7 (Fig. 1b and Table 1, main text), direct loadings from spray drift were assumed to occur in such link only, and in river segments intersecting apple orchards. The length of such segments was calculated by means of a shapefile intersection performed in QGIS Desktop 2.8.2 (QGIS, 2017) and

results are reported in Figure S2. Stream link 7 intercepted apple orchards belonging to Area 1 (yellow polygons in Fig. S2) for a total length of 1093 m, while apple orchards belonging to Area 2 (green polygons in Fig. S2) for a total length of 868 m. This means that, of the total stream link length (i.e., 10.34 km), about 1/5 is directly surrounded by apple orchards. A fixed river bed width of 10 m was assumed (based on field surveys) to calculate the surface water area and the spray drift loading to stream link 7. Equation 4 was parameterized selecting typical values for early applications on pome/stone fruit from FOCUS (2001b) and on the grounds of field observations. More specifically, the following values were assumed:

- z_1 and z_2 (distances from the edge of the treated field): 4 and 14 m (field observations)
- A, B, C, and D (regression parameters) 66.702, -0.7520, 3867.9, -2.4183 (FOCUS, 2001b)
- H (hinge distance): 11.4 (FOCUS, 2001b)

As a worst-case assumption, the chemical amount entering surface waters via spray drift was not subtracted from the chemical application rate (Table S4). Since in the Non Valley orchards low-drift nozzles are used to reduce the amount of pesticides lost via spray drift, a reduction by 50% of the calculated drift was applied. The resulting drift loading was assumed to entirely reach the water body, independently of wind direction; the calculation of wind-direction dependent drift loadings will be the object of a future improvement (e.g., as in Renaud et al., 2008).

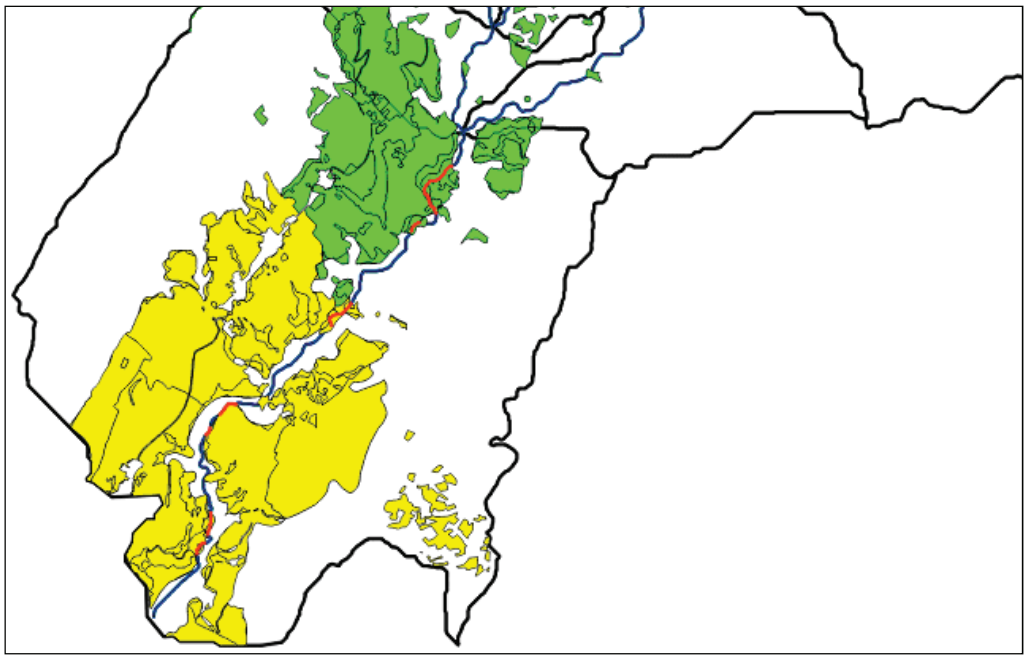

Figure S2. Focus on stream link 7 of the Novella River network, showing the areas (in red) in which the stream intercepts apple orchards. Apple orchards in yellow belong to Area 1, while those in green to Area 2 (for details, see 2.4.1 in the main text).

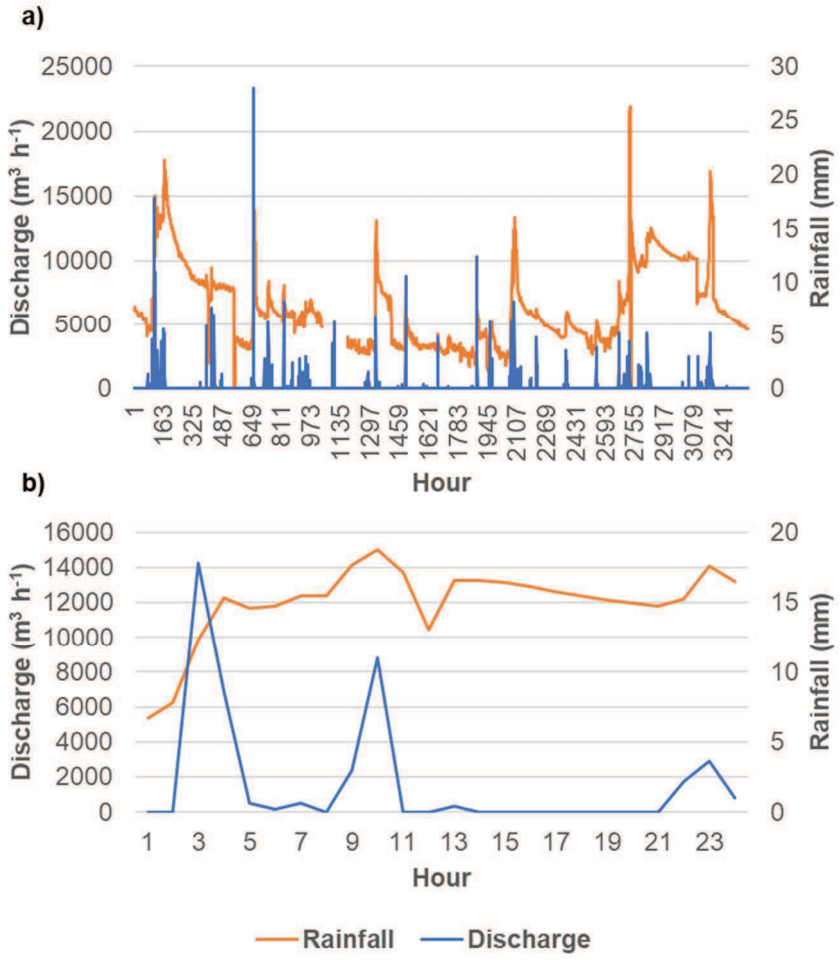

Figure S3. Relationship between hourly rainfall measured in Arsio and measured discharge (a) for the period June 5-October 24, 2012, for which discharge data were available; (b) for a single day (June 10, 2012).

Table S2. Physical-chemical properties at 25 °C and environmental half-lives for the three modelled chemicals. Values without superscript were taken from Mackay et al. (2006) for chlorpyrifos and Tomlin (1997) for pirimicarb and etofenprox.

Property	Unit	Chlorpyrifos	Pirimicarb	Etofenprox
MW	g mol^{-1}	350.6	283.3	376.49
MP	°C	42.75	90.5	37.2
VP	Pa	2.27E-03	9.7E-04	8.13E-07
WS	mg L^{-1}	0.73	3000 (20 °C)	2.25E-02
log K_{OW}	-	4.92	1.7	7.05
HLsoil	d	21 [a]	86 [a]	11 [a]
HLair	d	0.06 [b]	0.04 [c]	0.09 [d]
HLwat	d	5 [a]	33.3 [a]	5.7 [a]
HLsed	d	36.5 [a]	195 [a]	13.3 [a]
HLcrop	d	7 [a]	5.6 [a]	2.1 [a]

[a] PPDB, 2017
[b] EC, 2005
[c] EFSA, 2005
[d] EFSA, 2008

Table S3. Values for the non-time- and -space-variable environmental parameters and mass transfer coefficients adopted for the simulations with the integrated approach.

Parameter	Unit	Value
Sediment active layer depth	m	0.005 [a]
Aerosol particle concentration	μg m^{-3}	5 [a]
Aerosol dry deposition velocity	m h^{-1}	7.2 [b]
Scavenging ratio	-	200000 [b]
Volume fraction of sediment particles	-	0.1 [b]
Density of particles in water	kg m^{-3}	1500 [b]
Density of sediment particles	kg m^{-3}	1500 [b]
Density of air particles	kg m^{-3}	1500 [b]
OC fraction of suspended solids in water	-	0.038 [c]
OC fraction of sediment particles	-	0.038 [c]
Baseflow in order-1 links	m^3 h^{-1}	600 [a]
Volatilization MTC (air-side)	m h^{-1}	10 [d]
Volatilization MTC (water-side)	m h^{-1}	1 [d]
Sediment-water diffusion MTC	m h^{-1}	$1 \cdot 10^{-3}$ [d]
Sediment deposition rate	g m^{-2} d^{-1}	400 [d]
Sediment resuspension rate	g m^{-2} d^{-1}	200 [d]
Sediment burial rate	g m^{-2} d^{-1}	200 [d]

[a] Assumed as typical for rural areas (Mackay, 2001)
[b] Morselli et al. (2015)
[c] Assumed as equal to the average OC fraction in cultivated soils
[d] Morselli et al. (2014)

Table S4. Products, timings and rates of application for the three investigated substances for the productive season 2012. Area 1 refers to the southern part of the Novella River watershed (~ 830 ha), while Area 2 to the northern part (~ 500 ha). Data were provided by Edmund Mach Foundation (EMF, 2017).

Chlorpyrifos						
Date	**Area**	**Product (solid/liquid)**	**A.I. (g kg^{-1})**	**Dosage (g hL^{-1})**	**Solution (hL ha^{-1})**	**A.I. Use (kg ha^{-1})**
11-May-2011	2	Dursban 75 WG (solid)	750	75	15	0.84375
12-May-2011	1	ALISE' 75 WG (solid)	750	50	15	0.5625
17-May-2012	2	Dursban 75 WG (solid)	750	50	15	0.5625
18-May-2012	1	ALISE' 75 WG (solid)	750	50	15	0.5625
Pirimicarb						
Date	**Area**	**Product (solid/liquid)**	**A.I. (g kg^{-1})**	**Dosage (g hL^{-1})**	**Solution (hL ha^{-1})**	**A.I. Use (kg ha^{-1})**
29-Mar-2012	2	Aphox (solid)	175	200	15	0.525
Etofenprox						
Date	**Area**	**Product (solid/liquid)**	**A.I. (g L^{-1})**	**Dosage (mL hL^{-1})**	**Solution (hL ha^{-1})**	**A.I. Use (kg ha^{-1})**
24-Mar-2012	1	TREBON UP (liquid)	280	10	15	0.042
29-Mar-2012	2	TREBON UP (liquid)	280	25	15	0.105
2-Apr-2012	1	TREBON UP (liquid)	280	25	15	0.105

Text S4 - Soil sampling, measures and soil property assignation

While for cultivated soils data concerning soil texture and organic carbon (OC) fraction where available (EMF, 2017), a sampling campaign was carried out in September 2013 with the aim of preliminarily characterizing soil texture and OC in other areas of the watershed and for other land use types (forests and pastures; Fig. S3). Soils were sampled at six sites (two in mixed deciduous forests, three in coniferous forests and one in a pasture). For each sampling site, five sub-samples were collected on the vertices and at the middle of an imaginary square of 1 x 1 m through a soil core sampler. Soil samples were placed in bags, moved to a cooler and moved to the lab, where they were stored at -20 °C until texture and OC analysis.

Sand, clay and loam percentages were measured using the Pipette Method (D.M. n° 248 13/09/1999; IMA, 1999). Briefly, (1) soil samples were dried and sieved at 2 mm to separate the skeleton from the fine soil, (2) around 8 grams of sieved sample were stirred overnight in a solution with deionised water and sodium hexametaphosphate (dispersant), (3) such fraction was sieved at 200 µm and 100 µm to determinate sand fraction by filter weighting, (4) the remainder was put in a sedimentation cylinder to determine the silt and clay fractions by collecting samples with a known-volume pipette after the corresponding sedimentation time was passed. Soil OC was measured with the loss of ignition method. Briefly, soil samples (2 grams), were dried at 105 °C, weighed, put in a muffle furnace at 440°C for six hours and weighted again to determine the organic matter content (corresponding to the loss of weight after incineration). To convert organic matter (OM) into OC content, the relationship $OM = 1.724 \cdot OC$ was used. Results for soil texture and OC (%), expressed as averages of the five sub-samples, are reported in Table S5.

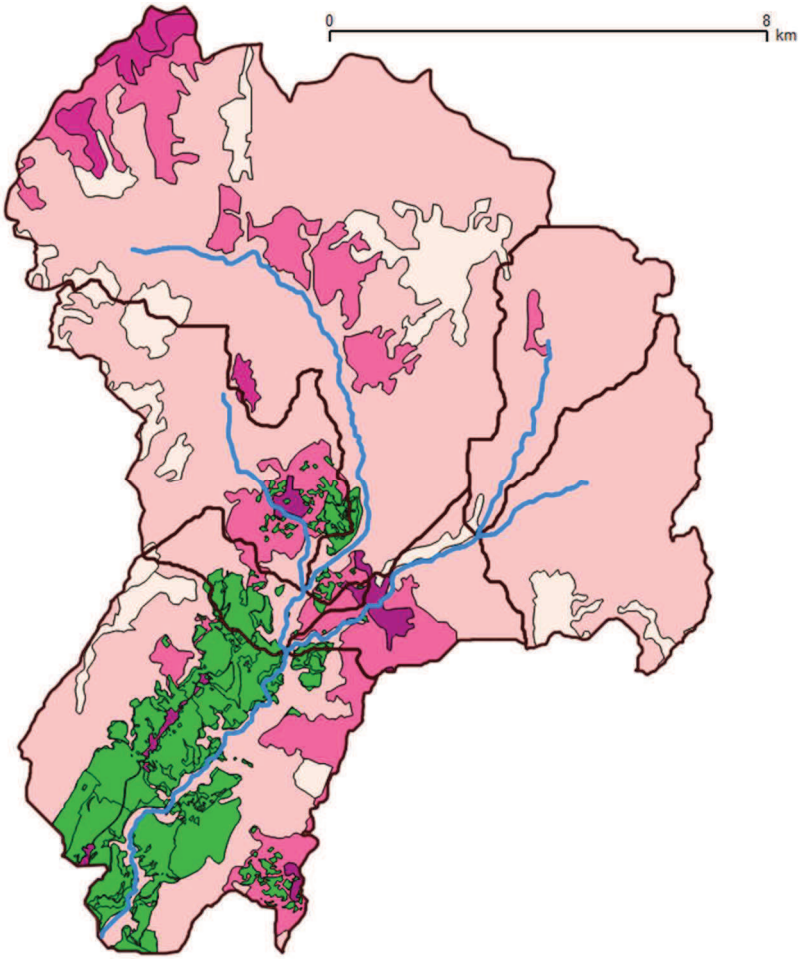

Figure S4. Distribution of the soil samples collected during the September 2013 campaign.

Table S5. Soil texture and OC and soil type attribution (Rawls et al., 1992) for the six samples.

Sample name	*Land cover*	*% Sand*	*% Silt*	*% Clay*	*OC %*	*Soil type*
BM1	Forest (mixed)	15.05	64.49	20.46	10.14	Silt loam
BM2	Forest (mixed)	58.98	32.47	8.55	12.9	Sandy loam
BC1	Forest (coniferous)	40.79	47.63	11.58	8.02	Loam
BC2	Forest (coniferous)	59.36	31.18	9.46	19.87	Sandy loam
BC3	Forest (coniferous)	61.68	36.29	2.03	20.21	Sandy loam
P1	Pasture	41.92	46.75	11.33	6.43	Loam

Soil texture and OC attribution in the SoilPlus input shapefile

For cultivated lands, textural data obtained from EMF (2017) were used to attribute texture to shapefile polygons. Soil type was in all cases loam or sandy loam and an average OC fraction of 0.038 ± 0.014 was measured. Data in EMF (2017) were reported according to municipality and the attribution of texture and OC to apple orchard polygons was therefore performed following this criterion, by means of a shapefile containing administrative municipality boundaries downloaded from GPTP (2017). For property attribution to soil polygons characterized by land uses other than orchard (i.e., forests, bush, other uncultivated areas, and urban), the data reported in Table S5 were used. More specifically, for pastures, the only pasture site sampled was assumed as representative of all pasture areas; for forest and bush areas, the closest sampled points were selected, while for uncultivated and urban areas the attribution simply followed a proximity criterion.

Text S5 - Surface runoff calibration and evaluation

To calibrate and evaluate surface runoff predictions, two river discharge datasets were used: a first one for the period July-October 2009 (Biasioni, 2010) and a second one (April-September 2012) presented in this work. In both cases, discharge was estimated starting from high-temporal resolution water level measurements performed at locations close to the water sampling station (see Fig. 1b, main text). The 2012 dataset was used for calibration purposes, while the 2009 one to test model performance. In 2012, eight episodes characterized by increase in discharge related to precipitation were selected and surface runoff was derived by integrating discharge peaks ad described in USDA-NRCS (2007). A comparison was then performed between surface runoff values obtained from discharge profiles and the surface runoff predicted by preliminary SoilPlus model runs for the same events. Results (Fig. S4) indicated that the model underestimated surface runoff for small rain amounts (daily rainfall amount < 10 mm d^{-1}), showed a good match for rain amounts between 10 and 25 mm d^{-1}, and overestimated surface runoff for higher rain amounts. Under/overestimations were up to one order of magnitude. Since the magnitude of under/overestimations appeared to be significantly related to rain amount (R^2 = 0.7689, P = 0.004334, n = 8; Fig. 4), a correction to the tabulated curve number in average moisture conditions (CN_2 in Equation 1) was applied. More specifically, CN_2 was multiplied by a factor equal to y, calculated using the equation reported in Figure S4 and the precipitation amount recorded in Arsio or Fondo (according to the sub-basin; EMF-GISU, 2017) as independent variable. To test model performance after calibration, nine rain events were selected from the 2009 discharge profile (Biasioni, 2010); predicted surface runoff was always within a factor of 2 to 4 with respect to measurements (results not shown), indicating a satisfying predictive ability.

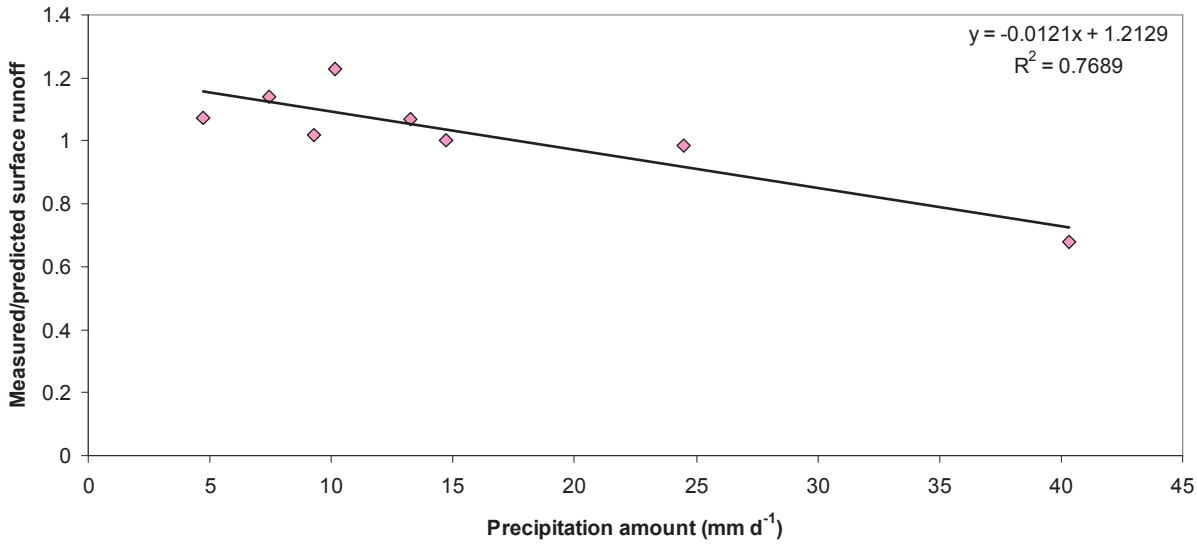

Figure S5. Relationship between the daily precipitation amount and the ratio between measured and predicted surface runoff for the eight events in 2012.

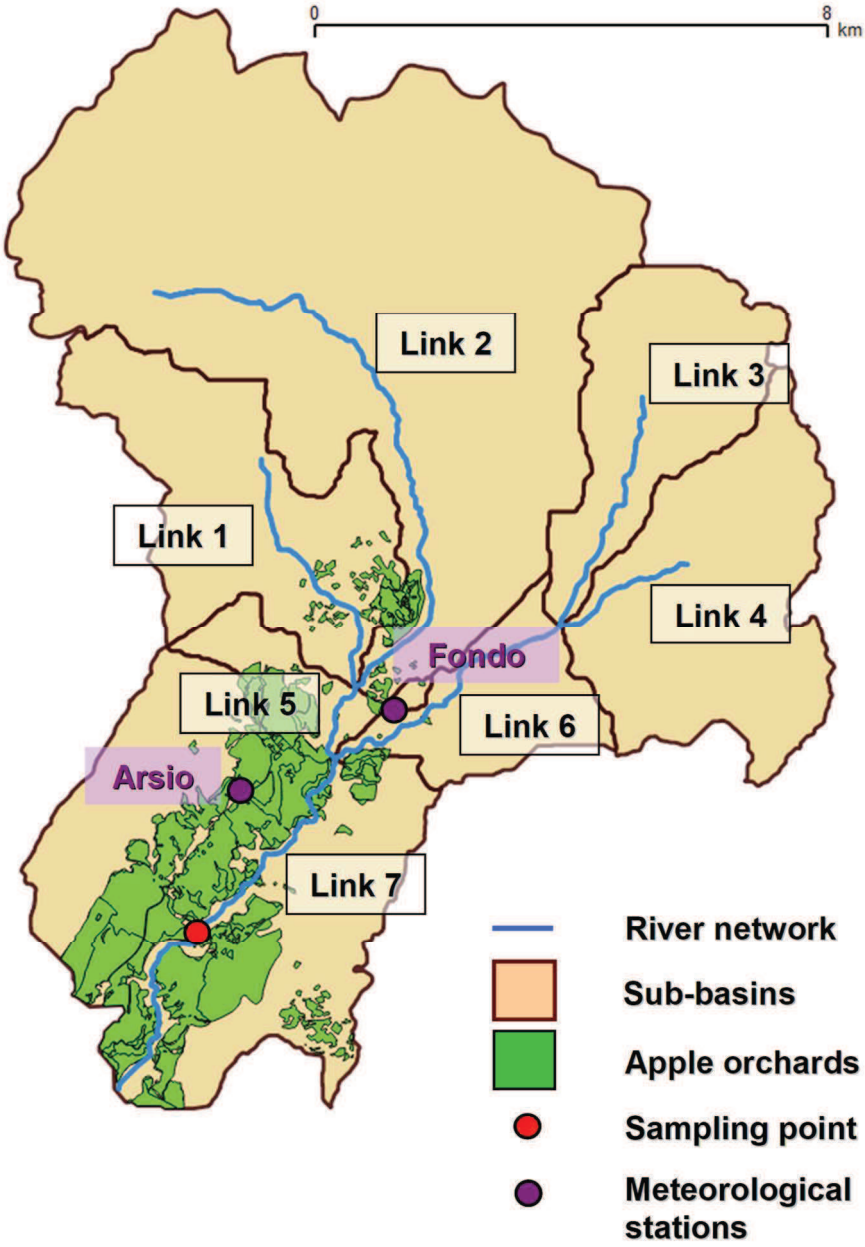

Figure S6. Meteorological stations selected for meteorological data attribution in the Novella River watershed (purple dots). The Arsio station was considered as representative of meteorology in sub-basin 7, while the Fondo station as representative of sub-basins 1 to 6.

Text S6 - Water temperature and suspended solids

The DynANet model requires hourly water temperature records as input. Since no measurements of such parameter were available for the Novella River during the simulation period, daily values were estimated through a linear relationship (R^2 = 0.7683, P = 1.93·10^{-3}, n = 7) between some water temperatures records taken in the Novella River during 2009 and 2010 (Biasioni, 2010; Ippolito, 2012) and the average air temperatures measured at the Romeno meteorological station during the same days (Meteotrentino, 2017). Such method is commonly used to overcome lack of data (e.g., Stefan and Preud d'homme, 1993; Erickson and Stefan, 1996). For water temperature estimation during the simulation period, the air temperatures measured in Arsio in 2011 and 2012 (EMF-GISU, 2017) were used. Minimum water temperature was set to 1.5 °C (slightly lower than the minimum value recorded in the river; Fig. S6). The resulting daily water temperatures are reported in Figure S7. To provide the input data for DynANet, temperatures were assumed as constant during the day.

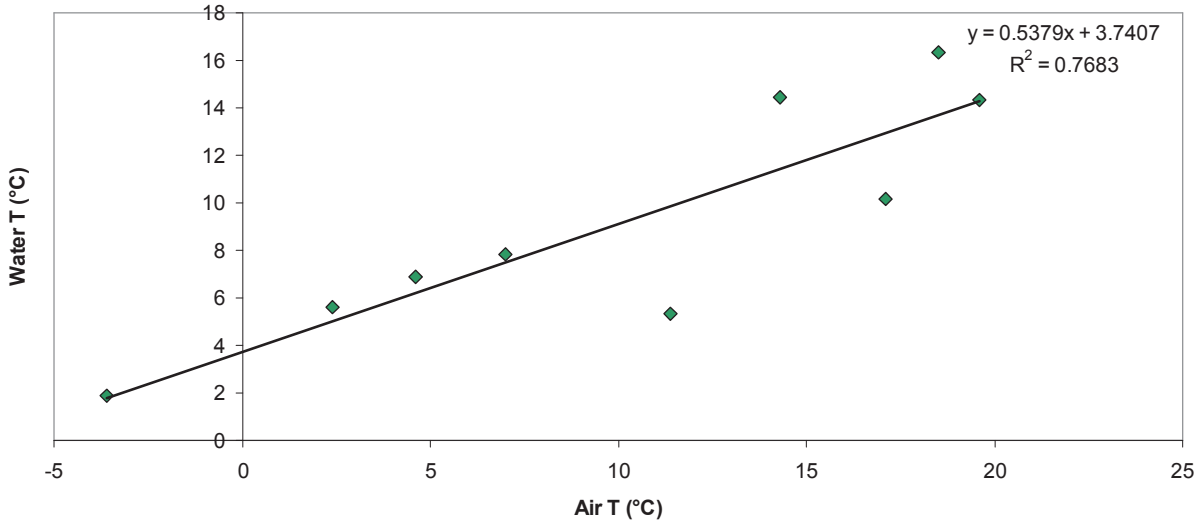

Figure S7. Relationship between air and water temperatures for the Novella River in 2009 and 2010 (Biasioni, 2010; Ippolito, 2012; Meteotrentino, 2017).

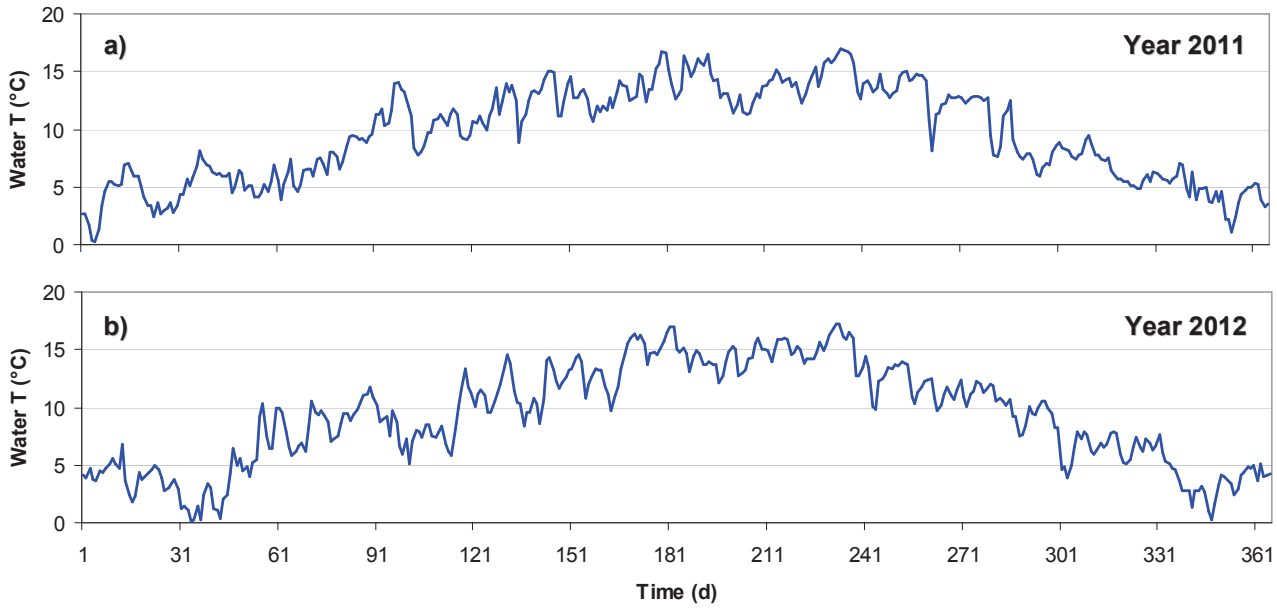

Figure S8. Daily water temperatures estimated for the years 2011 (chart a) and 2012 (chart b) starting from the daily average air temperatures measured in Arsio (EMF-GISU, 2017).

Similarly, a relationship between the suspended solid concentrations measured in the water samples collected in 2012 (Fig. S8; $R^2 = 0.6229$, $P < 0.00001$, $n = 27$) and the corresponding hourly rain amounts recorded in Arsio (EMF-GISU, 2017) was used to obtain the suspended solid temporal profiles (on an hourly basis) for all stream links in 2011 and 2012. For 2012, estimated values were then replaced by measurements, when available, with the aim of reducing the uncertainty in predictions water and particle-bound chemical fractions. Minimum suspended solid concentration was set to 50 mg L^{-1}. Results are reported in Figure S9. Since no information concerning OC fraction of suspended solids was available, a value of 0.05 (i.e., 5%) was assumed.

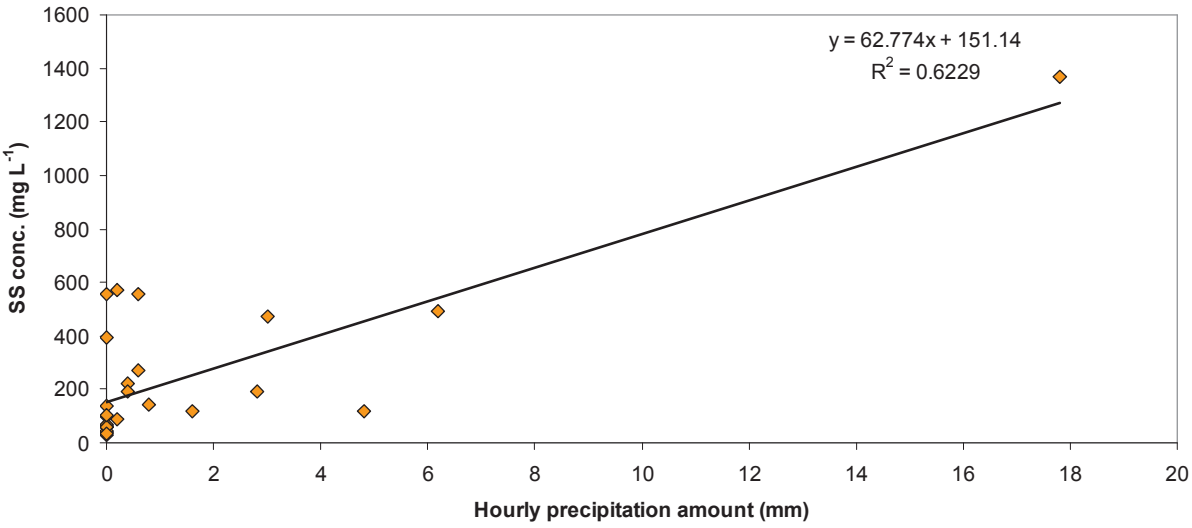

Figure S9. Relationship between the suspended solid concentrations measured in 2012 samples and the corresponding hourly rainfall amount measured in Arsio (EMF-GISU, 2017).

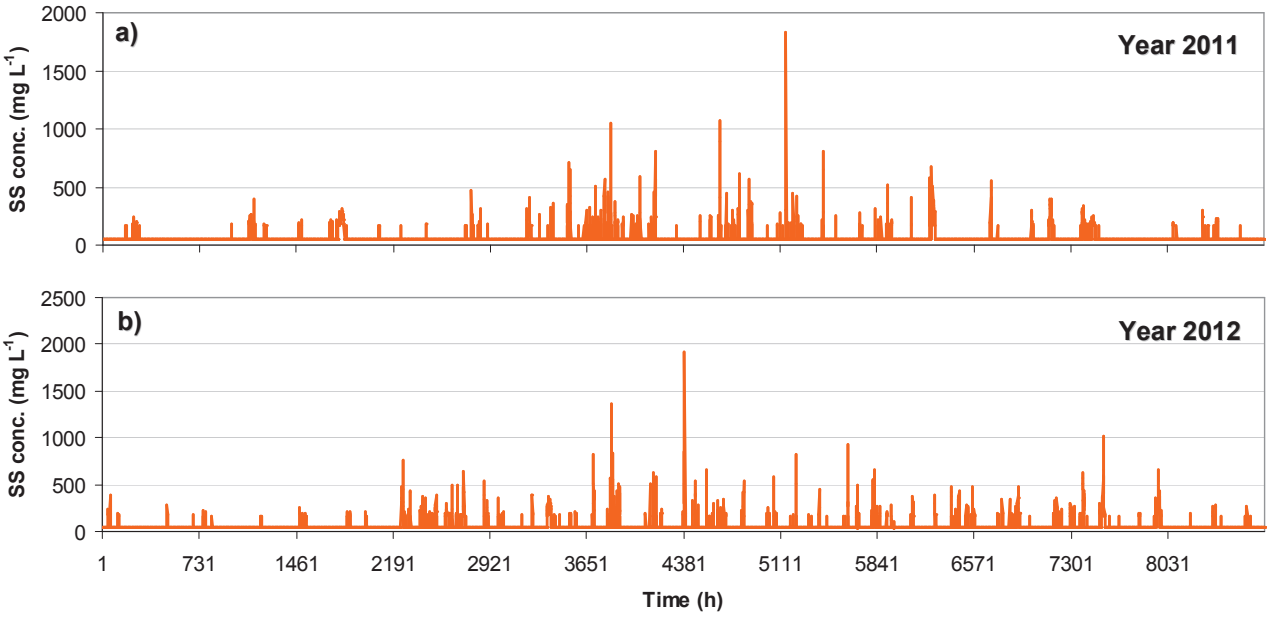

Figure S10. Hourly suspended solid concentrations estimated for the years 2011 (chart a) and 2012 (chart b) starting from the daily average air temperatures measured in Arsio (EMF-GISU, 2017).

Text S7 - Sensitivity analysis

A preliminary local sensitivity analysis (Augusiak et al., 2014) was conducted simulating the fate of three insecticides characterized by different hydrophobicity and persistence (chlorpyrifos, pirimicarb and etofenprox, Table S2). The maximum water-dissolved concentration predicted during a one-year simulation was selected as target, using as a reference the 2012 scenario described in section 2.4 of the main text. Tested parameters included chemical emission, physical-chemical properties, environmental half-lives, mass-transfer coefficients, water temperature and fluxes, compartment volumes and organic carbon fractions. Some of the parameters belonged to one of the two models only (e.g., OC fraction in soil, DOC concentration in soil water, albedo, altitude and latitude in SoilPlus or stream properties in DynANet), while physical-chemical properties and other parameters were common between the two models. The sensitivity analysis was performed by varying each parameter by 0.1% and calculating the influence of such variations on chemical water concentrations by assessing the index S (MacLeod et al., 2002):

$$|S| = \left| \frac{\Delta O / O}{\Delta I / I} \right| \tag{18}$$

where I is the input variable, O is the output of interest, and ΔI and ΔO are the variations in input and output parameters, respectively.

Table S6. Temporal series of samples collected by the autosampler ISCO 6712 in the Novella River during the period September 2011-September 2012.

ID	Date/time start	Date/time end	N° of samples	N° of analyzed samples
1	22-Sep-2011/10:39	23-Sep-2011/08:39	12	0 [a]
2	15-Apr-2012/16:36	16-Apr-2012/14:36	12	6
3	9-Jun-2012/15:02	10-Jun-2012/13:02	12	12
4	11-Jun-2012/15:27	12-Jun-2012/13:27	12	6
5	28-Jun-2012/11:15	29-Jun-2012/09:15	12	0 [a]
6	2-Jul-2012/18:25	3-Jul-2012/16:25	12	0 [b]
7	14-Jul-2012/01:06	14-Jul-2012/23:06	12	6
8	2-Ago-2012/20:04	3-Ago-2012/18:24	12	0 [a]
9	25-Ago-2012/21:16	26-Ago-2012/19:16	12	6
10	5-Sep-2012/19:21	6-Sep-2012/17:21	12	6

[a] Discarded since not representative of a runoff event ("false start" of ISCO)
[b] Discarded due to excessive delay between sampling and transfer to the lab

Table S7. Water, particle-phase and bulk concentrations (ng L^{-1}) of chlorpyrifos measured in the Novella River in 2011 and 2012. Where available, also suspended solids concentrations (SS) in water (mg L^{-1}) were reported. Manual samples are reported in red. When no suspended solid measures were available, bulk concentrations were assumed to match water phase ones.

Date	Time	Water c. (ng L^{-1})	Particle c. (ng L^{-1})	Bulk conc. (ng L^{-1})	SS (mg L^{-1})
17-May-2011	12:00 pm	21.6	n.a.	21.6	n.a.
3-Jun-2011	12:00 pm	5.3	n.a.	5.3	n.a.
28-Jun-2011	12:00 pm	4.5	n.a.	4.5	n.a.
13-Jul-2011	4:20 pm	3.8	n.a.	3.8	n.a.
13-Jul-2011	5:10 pm	5.0	n.a.	5.0	n.a.
13-Jul-2011	6:00 pm	8.9	n.a.	8.9	n.a.
13-Jul-2011	7:00 pm	5.3	n.a.	5.3	n.a.
13-Jul-2011	8:00 pm	5.0	n.a.	5.0	n.a.
13-Jul-2011	9:00 pm	8.1	n.a.	8.1	n.a.
13-Jul-2011	10:00 pm	18.3	n.a.	18.3	n.a.
14-Jul-2011	09:00 am	49.7	n.a.	49.7	n.a.
15-Apr-2012	4:36 pm	3.2	n.a.	3.2	n.a.
15-Apr-2012	8:36 pm	7.5	n.a.	7.5	n.a.
16-Apr-2012	00:36 am	3.3	n.a.	3.3	n.a.
16-Apr-2012	04:36 am	2.1	n.a.	2.1	n.a.
16-Apr-2012	08:36 am	2.3	n.a.	2.3	n.a.
16-Apr-2012	12:36 pm	1.8	n.a.	1.8	n.a.
9-Jun-2012	3:02 pm	532.4	941.7	1474.1	572.3
9-Jun-2012	5:02 pm	58.8	21.2	80.0	138.0
9-Jun-2012	7:02 pm	214.5	46.6	261.1	392
9-Jun-2012	9:02 pm	68.3	53.9	122.1	58.0
9-Jun-2012	11:02 pm	89.8	30.0	119.8	38.7
10-Jun-2012	01:02 am	576.5	691.6	1268.1	1368.3
10-Jun-2012	03:02 am	331.2	218.9	550.0	554.7
10-Jun-2012	05:02 am	31.5	104.4	135.9	272.0
10-Jun-2012	07:02 am	337.7	127.3	465.0	471.7
10-Jun-2012	09:02 am	47.4	45.0	92.4	557.3
10-Jun-2012	11:02 am	31.5	26.4	57.9	220.0
10-Jun-2012	1:02 pm	21.0	16.2	37.2	100.5
11-Jun-2012	3:27 pm	126.7	14.5	141.2	192.2
11-Jun-2012	7:27 pm	87.1	n.a.	87.1	n.a.
11-Jun-2012	11:27 pm	59.5	3.39	62.9	89.2
12-Jun-2012	03:27 am	85.2	4.61	89.8	120.2

12-Jun-2012	07:27 am	207.5	n.a.	207.5	n.a.
12-Jun-2012	11:27 am	96.4	n.a.	96.4	n.a.
14-Jul-2012	01:06 am	8.9	n.a.	8.9	n.a.
14-Jul-2012	05:06 am	5.1	n.a.	5.1	n.a.
14-Jul-2012	09:06 am	27.3	n.a.	27.3	n.a.
14-Jul-2012	5:06 pm	3.3	n.a.	3.3	n.a.
14-Jul-2012	9:06 pm	1.1	n.a.	1.1	n.a.
15-Jul-2012	11:06 pm	4.7	n.a.	4.7	n.a.
25-Aug-2012	9:16 pm	2.1	7.9	10.0	144.2
26-Aug-2012	01:16 am	41.6	83.8	125.4	492.9
26-Aug-2012	05:16 am	10.4	15.9	26.3	61.9
26-Aug-2012	09:16 am	2.2	41.3	43.5	28.8
26-Aug-2012	1:16 pm	21.1	18.8	20.9	190.3
26-Aug-2012	5:16 pm	5.8	22.4	28.2	43.9
5-Sep-2012	7:21 pm	6.2	16.4	22.6	119.2
5-Sep-2012	11:21 pm	3.3	9.7	13.0	66.6
6-Sep-2012	03:21 am	6.8	6.9	13.7	60.9
6-Sep-2012	07:21 am	0.9	8.5	9.4	58.6
6-Sep-2012	11:21 am	1.1	3.3	4.4	104.9
6-Sep-2012	3.21 pm	0.7	n.d.	0.7	36.9

n.d.: not detected, n.a.: not available. Detection limits were 0.1 ng L^{-1} for water concentrations and 1-40 ng L^{-1} (according to suspended solid amount) for particle-phase concentrations.

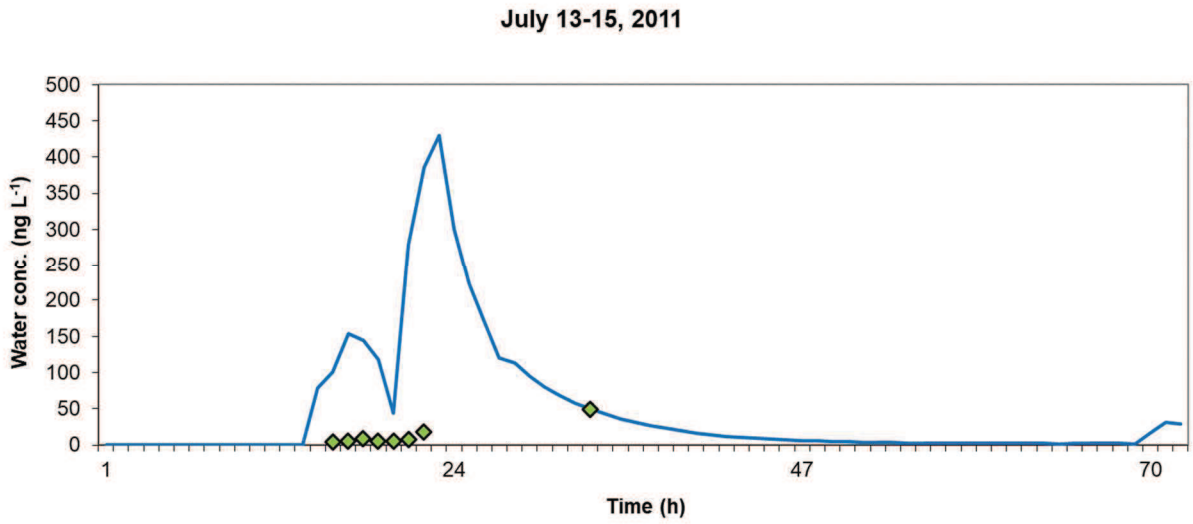

Figure S11. Chlorpyrifos water concentrations (ng L^{-1}) in stream link 7 as predicted by DynAPlus from July 13 to 15, 2011 (lines) and corresponding measured values (markers).

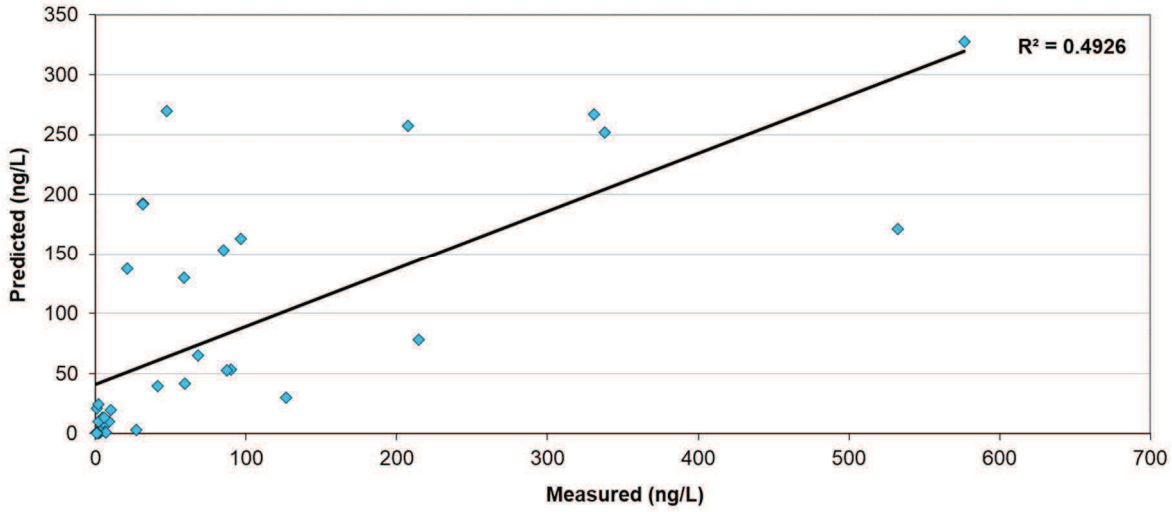

Figure S12. Relationship between measured (*x*-axis) and predicted (*y*-axis) chlorpyrifos concentrations during the year 2012 (R^2 = 0.4926, P < 0.00001, n = 36).

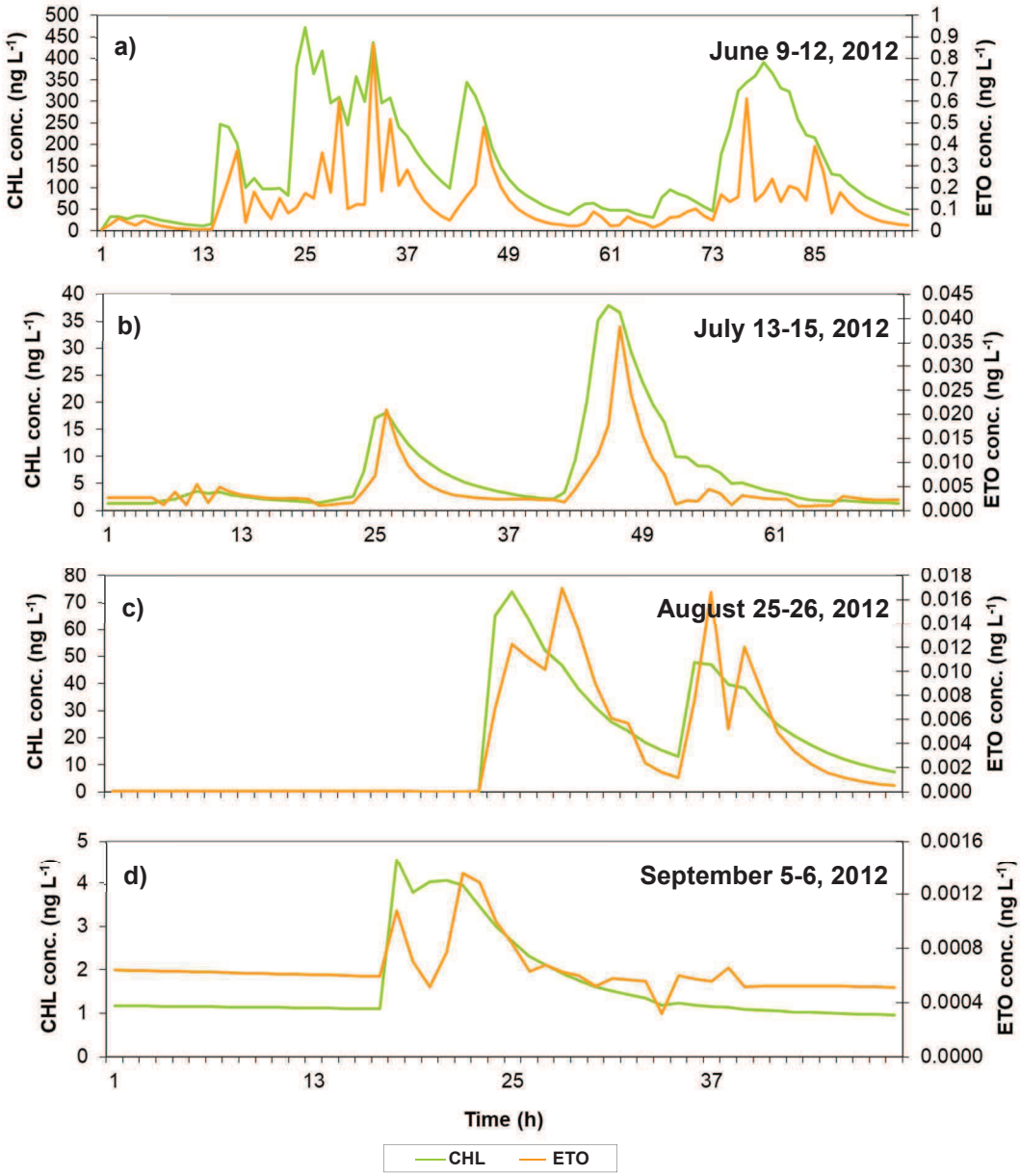

Figure S13. Comparison between chlorpyrifos (CHL; primary *y*-axis) and etofenprox (ETO; secondary *y*-axis) water concentrations (ng L^{-1}) for the five runoff events also investigated in model evaluation (see 3.2 and Fig. 4, main text). The first two events are condensed in Figure S12a. Pirimicarb concentrations are not reported since predicted water concentrations are extremely low ($1 \cdot 10^{-10}$ ng L^{-1}) already during the June events.

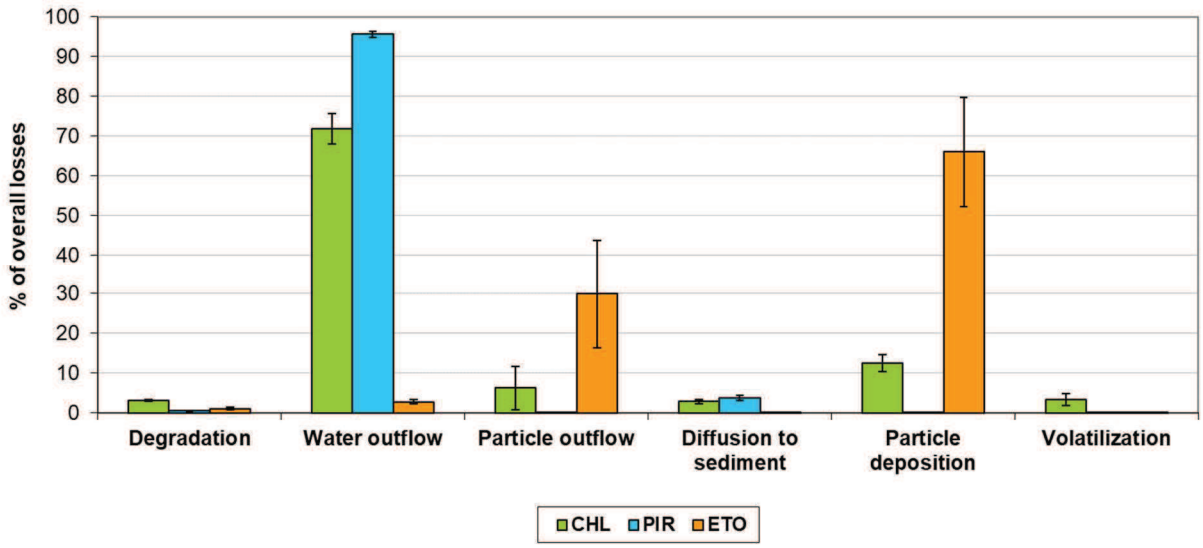

Figure S14. Relative importance of the different loss processes with respect to the overall losses from the water compartment (%) in stream link 7 for the three model chemicals during the simulation period (year 2012). Bars represent standard deviations (relative importance was first investigated on an hourly basis, and annual averages and standard deviations were then computed for each process and chemical).

Text S8 - Sensitivity analysis

Figure S14 depicts the results of the sensitivity analysis performed for chlorpyrifos (CHL), pirimicarb (PIR) and etofenprox (ETO). For all chemicals, the most influential parameter was curve number (*CN*), with an *S* index of 1.6 for CHL and even > 15 for PIR and ETO. This result confirmed expectations, since *CN* determines the amount of runoff water and thus chemical runoff, which represents a direct input to surface waters. Similarly, for PIR and ETO, rainfall amount (*Rainfall*) was the second most influential variable (*S* = 1.4 and 3.01, respectively), while for CHL the same parameter was of lower importance (*S* = 0.12). The higher sensitivity of PIR and ETO water concentrations (with respect to CHL ones) to *CN* and *Rainfall* can be ascribed to physical-chemical properties: more specifically, the high PIR water solubility (3000 mg L^{-1} at 20 °C) and low hydrophobicity (log K_{OW} = 1.7) and, in contrast, the high hydrophobicity of ETO (log K_{OW} = 7.05), significantly enhance their mobility mediated by runoff water (for PIR) and DOC moving with runoff water (for ETO). This last observation is also confirmed by the high *S* score obtained for the DOC concentration in soil water (*DOC conc*) for the hydrophobic insecticide ETO (*S* = 0.97); this parameter showed a slightly lower score for CHL (*S* = 0.61), while for the polar insecticide PIR it was totally not influential. ETO concentrations were also highly affected by half-life in soil (*HLsoil*; *S* = 1.14) and OC fraction of suspended particles (*OCfr*; *S* = 0.96); the latter parameter was important also for CHL (*S* = 0.27). Application rate (*app rate*) and depth (*app depth*) followed (*S* = 1 for all chemicals). CHL showed an intermediate behaviour between PIR and ETO; its water concentrations were mostly influenced by OC fraction in soil (*OC*fr) and stream link water volume (determined by link length *LinkL* and bottom width *BottomW*; *S* = 0.73 and 0.27, respectively). The latter parameters showed similar importance for PIR but were not influential for ETO.

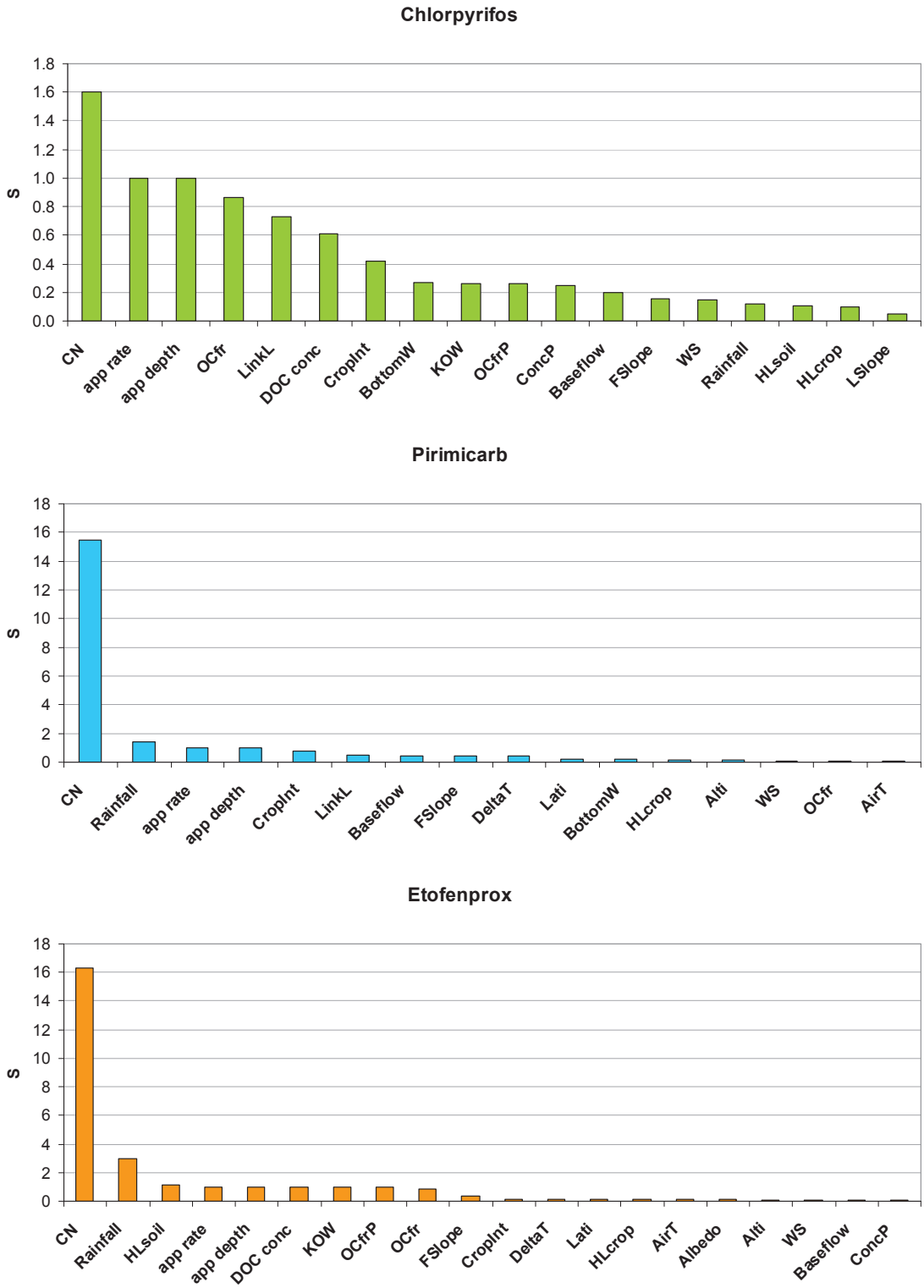

Figure S15. Sensitivity analysis results for the three investigated chemicals. Parameters are reported for each chemical in decreasing S order. Only those with $S \geq 0.05$ were included.

Average polygon slope (*FSlope*) was among the most influential parameters for all test chemicals (S = 0.40 for PIR, 0.35 for ETO, 0.16 for CHL), highlighting the importance of the improvement made to the SoilPlus model by adding a slope correction to curve number (see Text S1). Similarly, the fraction of applied chemical intercepted by crop (*CropInt*) showed high S scores for all pesticides (0.8 for PIR, 0.42 for CHL, 0.17 for ETO). Being a local sensitivity analysis (i.e., one parameter was slightly varied a little at a time), the effort presented here did not allow capturing, for example, the effect of the interactions between parameters (Augusiak et al., 2014); however, it helped in the identification of the crucial inputs (chemical properties and environmental system descriptors), to which particular attention should be paid in order to obtain accurate results. To summarize results, S scores obtained for the three chemicals were averaged; variables were then sorted to identify the most influential parameters. Results are reported in Figure S15. The six most influential parameters ($S \geq$ 0.5) were curve number, rainfall amount, application rate and depth, OC fraction in soil and DOC concentration in soil water.

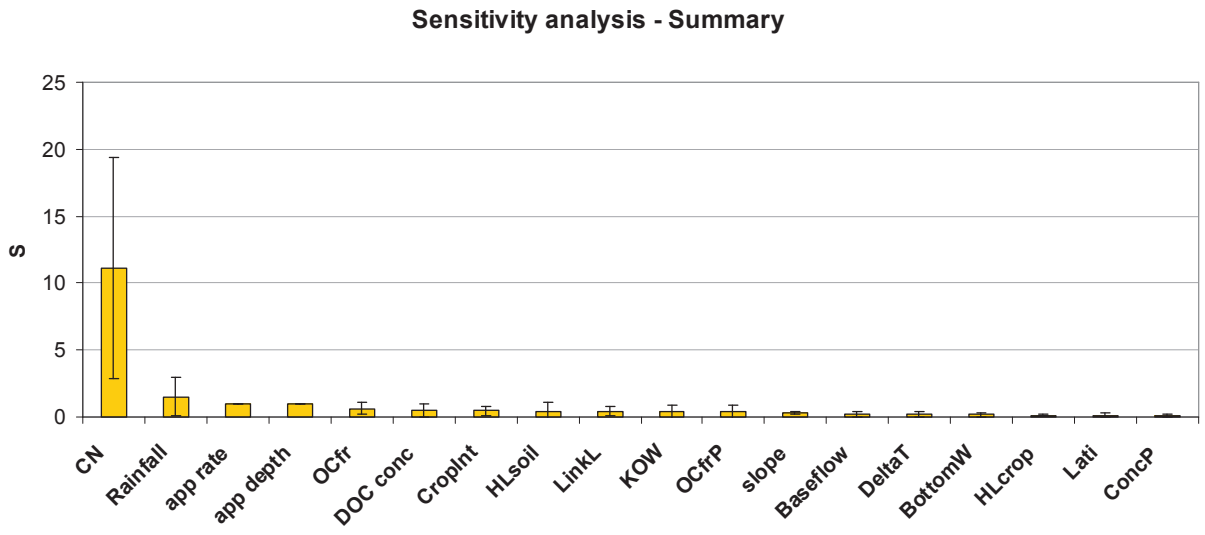

Figure S16. Summary of the average *S* scores (with standard deviations) for the most influential parameters, reported in decreasing *S* order. Only parameters with average $S \geq 0.1$ were included.

Tested parameters were: application rate (kg ha^{-1}, *app rate*) and depth (m, *app depth*), water solubility (mg L^{-1}, *WS*), vapour pressure (Pa, *VP*), melting point (°C, *MP*), octanol-water partition coefficient (dimensionless, K_{OW}), chemical half-life in soil (d, *HLsoil*), air (d, *HLair*), water (d, *HLwat*), sediment (d, *HLsed*), and crop (d, *HLcrop*), crop interception (unitless, *CropInt*), OC fraction in soil (unitless, *OCfr*), soil OC half-life (d, *HLOC*), DOC concentration in soil water (mg L^{-1}, *DOC conc*), average polygon slope (m m^{-1}, *FSlope*), soil bulk density (g cm^{-3}, *BulkDen*), soil total porosity (cm^3 cm^{-3}, *TotPor*), field capacity (cm^3 cm^{-3}, *FC*), wilting point (cm^3/ cm^{-3}, *WP*), curve number (unitless, *CN*), albedo (unitless, *Albedo*), altitude (m, *Alti*), latitude (°, *Lati*), yearly delta temperature (°C, *DeltaT*), rainfall amount (mm, *Rainfall*), global solar radiation (MJ m^{-2}, *Radi*), lower-air compartment height (m, *HeightLA*), lower-air compartment wind speed (m s^{-1}, *WSpeedLA*), air temperature (°C, *AirT*), link length (m, *LinkL*), link average slope (m m^{-1}, *LSlope*), link bottom width (m, *BottomW*), stream baseflow (m^3 h^{-1}, *Baseflow*), water temperature (°C, *WatT*), sediment depth (m, *SedD*), volume fraction of solids in sediment (unitless, *VFSed*), OC fraction in sediment solids (unitless, *OCfrSedP*), suspended solid concentration in water (mg L^{-1}, *ConcP*), OC fraction in suspended particles (untiless, *OCfrP*).

References

Augusiak, J., Van den Brink, P.J., Grimm, V., 2014. Merging validation and evaluation of ecological models to 'evaludation': a review of terminology and a practical approach. Ecol. Model. 280, 117–128 (http://dx.doi.org/10.1016/j.ecolmodel.2013.11.009).

Biasioni, D., 2010. Analisi delle portate Rio Sass e Torrente Novella. Internal report, Dambel Municipality, Trento, Italy.

EC (European Commission), 2005. Review report for the active substance chlorpyrifos. Brussels: European Commission. Health and Consumer Protection Directorate-General. EC Document Reference SANCO/3059/99 - rev. 1.5 (http://ec.europa.eu/food/plant/pesticides/eu-pesticides-database/public/?event=activesubstance.ViewReview&id=138).

EFSA (European Food Safety Authority), 2005. Conclusion regarding the peer review of the pesticide risk assessment of the active substance pirimicarb. EFSA Scientific Report (2005) 43, 1–76 (https://www.efsa.europa.eu/en/efsajournal/pub/rn-43).

EFSA (European Food Safety Authority), 2008. Conclusion regarding the peer review of the pesticide risk assessment of the active substance etofenprox. EFSA Scientific Report (2008) 213, 1–131 (http://www.efsa.europa.eu/it/efsajournal/pub/213r).

EMF (Edmund Mach Foundation), 2017. Edmund Mach Foundation website: http://www.fmach.it/.

EMF-GISU (Edmund Mach Foundation - Geographic Information System Unit), 2017. Edmund Mach Foundation, Geographic Information System Unit website: http://meteo.iasma.it/meteo/.

Erickson, T.R., Stefan, H.G., 1996. Correlations of Oklahoma stream temperatures with air temperatures. Project Report n. 398. University of Minnesota, St. Anthony Falls Laboratory, Minneapolis, Minnesota.

FOCUS (FOrum for Co-ordination of pesticide fate models and their USe), 2001a. FOCUS Surface Water Scenarios in the EU Evaluation Process under 91/414/EEC.Report of the FOCUS Working Group on Surface Water Scenarios. EC Document Reference SANCO/4802/2001-rev2. 245 pp. http://esdac.jrc.ec.europa.eu/projects/focus-dg-sante.

FOCUS (FOrum for Co-ordination of pesticide fate models and their USe), 2001b. APPENDIX B - Parameterization of spray drift input.

Google Maps, 2017. Google Maps website: https://www.google.it/maps.

Huang, M., Gallichand, J., Wang, Z., Goulet, M., 2006. A modification to the Soil Conservation Service curve number method for steep slopes in the Loess Plateau of China. Hydrol. Process. 20 (3), 579–589 (http://dx.doi.org/10.1002/hyp.5925).

Ippolito, A., 2012. Plant protection product risk assessment for aquatic ecosystems evaluation of effects in natural communities. PhD thesis. University of Milano Bicocca, Milan.

IMA (Italian Ministry of Agriculture), 1999. D.M. n° 248 13/09/1999. Decreto Legislativo n° 248 del 1999 "Metodi ufficiali di analisi chimica del suolo", Ministro per le Politiche Agricole, Gazz. Uff. Suppl. Ordin. N° 248 del 21/10/1999.

Jarrett, R.D., 1984. Hydraulics of high-gradient streams. J. Hydraul. Eng. 110 (11), p. 1519–1539 (https://doi.org/10.1061/(ASCE)0733-9429(1984)110:11(1519)).

Mackay, D., 2001. Multimedia Environmental Models: The Fugacity Approach. second ed. Boca Raton, Lewis Publishers.

Mackay, D., Mackay, D. (Eds.), 2006. Handbook of physical-chemical properties and environmental fate for organic chemicals, 2nd ed. Volume IV, Chapter 18: Insecticides. Taylor & Francis Group: Boca Raton.

MacLeod, M., Fraser, A.J., Mackay, D., 2002. Evaluating and expressing the propagation of uncertainty in chemical fate and bioaccumulation models. Environ. Toxicol. Chem. 21 (4), 700–709 (http://dx.doi.org/ 10.1002/etc.5620210403).

Meteotrentino, 2017. Meteotrentino website: http://www.meteotrentino.it/.

Morselli, M., Semplice, M., De Laender, F., Van den Brink, P.J., Di Guardo, A., 2015. Importance of environmental and biomass dynamics in predicting chemical exposure in ecological risk assessment. Sci. Total Environ. 526, 338–345 (http://dx.doi.org/10.1016/j.scitotenv.2015.04.072).

Morselli, M., Semplice, M., Villa, S., Di Guardo, A., 2014. Evaluating the temporal variability of concentrations of POPs in a glacier-fed stream food chain using a combined modeling approach. Sci. Total Environ. 493, 571–579 (http://dx.doi.org/10.1016/j.scitotenv.2014.05.150).

Neitsch, S.L., Arnold, J.G., Kiniry, J.R., Williams, J., 2005. Soil Water Assessment Tool Theoretical Documentation (https://oaktrust.library.tamu.edu/bitstream/handle/1969.1/128050/TR-

406_Soil%20and%20Water%20Assessment%20Tool%20Theoretical%20Documentation.pdf?sequence=1&isAllowed=y).

GPTP (Geographic Portal of Trento Province), 2017. Geographic Portal of Trento Province website: http://www.territorio.provincia.tn.it/portal/server.pt/community/portale_geocartografico_trentino/254.

PPDB (Pesticides Properties DataBase), 2017. University of Hertfordshire, Pesticide Properties Database website: http://sitem.herts.ac.uk/aeru/ppdb/en/.

QGIS, 2017. QuantumGIS website: https://www.qgis.org/it/site/.

Rawls, W. J., Ahuja, L. R., Brakensiek, D. L., Shirmohammadi, A., 1992. Infiltration and soil water movement. In Handbook of Hydrology; Maidment, D. R., Ed.; McGraw-Hill Inc.: New York, 5.1-5.51.

Renaud, F.G., Bellamy, P.H., Brown, C.D., 2008. Simulating pesticides in ditches to assess ecological risk (SPIDER): I. Model description. Sci. Total Environ. 394 (1), 112–123. (http://dx.doi.org/10.1016/j.scitotenv.2007.11.038).

SCS (Soil Conservation Service), 1972. SCS National Engineering Handbook, Section 4, Hydrology. Washington, D.C., U.S.

Sharpley, A.N., Williams, J.R., 1990. EPIC Erosion/Productivity Impact Calculator: 1. Model Documentation. USA Department of Agriculture Technical Bulletin No. 1768, USA Government Printing Office, Washington DC.

Stefan, H.G., Preud'homme, E.B., 1993. Stream temperature estimation from air temperature. J. Am. Water Resour. Assoc. 29, 27–45 (http://10.1111/j.1752-1688.1993.tb01502.x).

Strahler, A.N., 1952. Hypsometric (area-altitude) analysis of erosional topography. Geol. Soc. Am. Bull. 63 (11), 1117–1142 (http://dx.doi.org/10.1130/0016-7606(1952)63[1117:HAAOET]2.0.CO;2).

Tomlin, C. (ed), 1997. The Pesticide Manual: Eleventh Edition. Crop Protection Publications, British Crop Protection Council and the Royal Society of Chemistry. United Kingdom.

Trento Province, 2017. Trento Province, Urban Planning website: http://www.urbanistica.provincia.tn.it/.

USDA (United States Department of Agriculture)-NRCS (Natural Resources Conservation Service), 2007. National Engineering Handbook, Part 630, Hydrology.

Williams J.R., 1969. Flood routing with variable travel time or variable storage coefficient. Transaction of the ASABE 12 (1), 100–103.

Paper II: How good are the predictions of mobility of aged polychlorinated biphenyls (PCBs) in soil? Insights from a soil column experiment

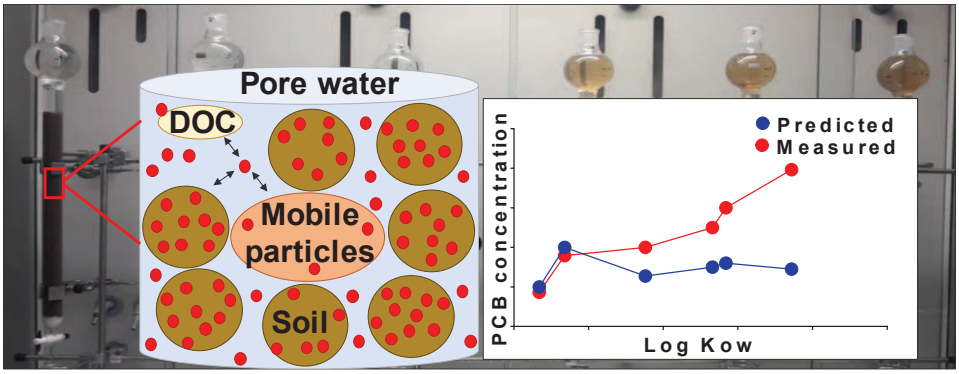

Chiara Maria Vitale, Elisa Terzaghi, Dario Zati, and Antonio Di Guardo*

Department of Science and High Technology (DiSAT), University of Insubria, Via Valleggio 11, Como, Italy

Science of The Total Environment 645 (2018), 865–875

* Corresponding author.